Correlation between High Resolution Dynamic MR Features and Prognostic Factors in Breast Cancer

Shin Ho Lee, MD
Nariya Cho, MD
Seung Ja Kim, MD
Joo Hee Cha, MD[2]
Kyung Soo Cho, MD
Eun Sook Ko, MD
Woo Kyung Moon, MD

Index terms:
Breast neoplasms
Breast, MR
Prognostic factors

DOI:10.3348/kjr.2008.9.1.10

Korean J Radiol 2008;9:10-18
Received October 2, 2006; accepted after revision May 7, 2007.

[1]Department of Radiology, Seoul National University College of Medicine and Institute of Radiation Medicine, Seoul National University Medical Research Center, Seoul 110-744, Korea; [2]Department of Radiology, Seoul Municipal Boramae Hospital, Seoul 156-707, Korea

This study was supported by a grant (A062260) from the Innovative Research Institute for Cell Therapy, Republic of Korea.

Address reprint requests to:
Woo Kyung Moon, MD, Department of Radiology, Seoul National University College of Medicine and Institute of Radiation Medicine, Seoul National University Medical Research Center, 28, Yongon-dong, Chongno-gu, Seoul 110-744, Korea.
Tel. (822) 2072-2584
Fax. (822) 743-6385
e-mail: moonwk@radcom.snu.ac.kr

Objective: To correlate high resolution dynamic MR features with prognostic factors in breast cancer.

Materials and Methods: One hundred and ninety-four women with invasive ductal carcinomas underwent dynamic MR imaging using T1-weighted three-dimensional fast low-angle shot (3D-FLASH) sequence within two weeks prior to surgery. Morphological and kinetic MR features were determined based on the breast imaging and reporting data system (BI-RADS) MR imaging lexicon. Histological specimens were analyzed for tumor size, axillary lymph node status, histological grade, expression of estrogen receptor (ER), expression of progesterone receptor (PR), and expression of p53, c-erbB-2, and Ki-67. Correlations between the MR features and prognostic factors were determined using the Pearson χ^2 test, linear-by-linear association, and logistic regression analysis.

Results: By multivariate analysis, a spiculated margin was a significant, independent predictor of a lower histological grade ($p < 0.001$), and lower expression of Ki-67 ($p = 0.007$). Rim enhancement was significant, independent predictor of a higher histological grade ($p < 0.001$), negative expression of ER ($p = 0.001$), negative expression of PR ($p < 0.001$) and a larger tumor size ($p = 0.006$). A washout curve may predict a higher level of Ki-67 ($p = 0.05$). Most of the parameters of the initial enhancement phase cannot predict the status of the prognostic factors. Only the enhancement ratio may predict a larger tumor size ($p = 0.05$).

Conclusion: Of the BI-RADS-MR features, a spiculated margin may predict favorable prognosis, whereas rim enhancement or washout may predict unfavorable prognosis of breast cancer.

Dynamic contrast-enhanced magnetic resonance (MR) imaging has emerged as a promising modality for the detection, diagnosis, and staging of breast cancer. MR imaging provides important information not only on the morphology of lesions but also on the functional aspects reflected by the temporal and spatial uptake of contrast medium. Integration of both kinetic and morphological features is important for accurate diagnosis (1, 2). In addition to these roles, the relationship of MR features and prognostic factors of breast cancer recently have been studied. However, these studies showed various results that might be due to variable MR techniques and interpretation criteria (3−11). Moreover, to the best of our knowledge, there has been only one study to correlate the MR features based on the breast imaging and reporting data system (BI-RADS)-MR imaging lexicon (12) with prognostic factors of breast cancer, but the study did not correlate various early phase kinetic parameters (13).

The purpose of this study was to correlate MR features of invasive ductal carcinomas

according to the BI-RADS-MR imaging lexicon with prognostic factors including tumor size, axillary lymph node status, histological grade, estrogen receptor (ER), progesterone receptor (PR), p53, c-erbB-2, and Ki-67.

MATERIALS AND METHODS

Patients

Between March 2004 and November 2004, 270 consecutive patients with a histopathologically confirmed invasive ductal carcinoma not otherwise specified (NOS) underwent MR imaging within two weeks prior to surgery. Due to having undergone a previous excisional biopsy, 47 patients were excluded and 29 patients were excluded due to previous neoadjuvant chemotherapy. The remaining 194 patients (age range 29−76 years, mean 47 years) constituted the study group. In patients with multifocal, multicentric carcinoma, the largest lesion was analyzed. The institutional review board of our institution approved the study and informed consent was obtained from all patients.

MR Imaging

MR imaging was performed with a 1.5 T imager (Sonata; Siemens Medical Systems, Erlangen, Germany). The affected side of each patient was examined by using a dedicated double-breast coil, with the patient in a prone position. Dynamic contrast-enhanced images with one precontrast and four post-contrast series were obtained, using a T1-weighted three-dimensional fast low-angle shot (3D-FLASH) sequence with fat suppression in a one-sided sagittal plane (TR 4.9 ms, TE 1.8 ms, flip angle 12°, field of view 170 mm, matrix 224×448, time of acquisition 84 seconds, 1.0 mm section thickeness with no gap). A bolus of gadopentetate dimeglumine (Magnevist; Schering, Berlin, Germany) was injected intravenously by hand at a dose of 0.1 mmol per kilogram of body weight within 15 seconds, followed by a 20 mL saline solution flush.

Image Analysis

Post-processing subtraction of the dynamic images was performed for all patients. We obtained two different series of subtracted images for each patient: images obtained before the administration of contrast material were subtracted from the early phase (84 seconds) images obtained after the administration of contrast material, and delayed phase (336 seconds) images were subtracted from the early phase postcontrast images. The first set of the subtracted images showed early enhancement of the lesions, and the second set showed temporal changes in the enhancement pattern between each pair of early and delayed phase images.

Two breast radiologists who were blinded to other information retrospectively analyzed the images by consensus according to the BI-RADS-MR imaging lexicon. Abnormal enhancement was classified as mass or non-mass enhancement. The shape of a mass was described as round, oval, lobulated, or irregular. The margin of a mass was described as smooth, irregular, or spiculated. The internal enhancement pattern of a mass was described as homogeneous, heterogeneous, or rim enhancement. Signal intensities were obtained from the precontrast and each postcontrast series using operator-defined regions of interest (ROI). Measurement was performed in at least three areas within the tumor and the maximally enhancing ROI was selected for analysis. The smallest possible pixel size (four pixels) was used for the ROIs. The parameters of MR kinetics were the enhancement ratio (signal intensity after contrast injection−baseline signal intensity/baseline signal intensity ×100%), the peak time, the initial slope (enhancement ratio/peak time), and the type of enhancement curve. The curve shape rather than the absolute value of the enhancement distinguished the type of enhancement curve. The shape of the enhancement curve was described as persistent, plateau, and washout. A persistent curve was continuous enhancement increasing with time. A plateau curve showed maximal signal intensity approximately 2 to 3 minutes after injection, and the signal intensity remained constant at this level. A washout curve showed decreasing signal intensity within 2 to 3 minutes after peak enhancement.

Histopathological Analysis

Histopathological features were analyzed by one pathologist with 20 years of experience in the practice of breast pathology. The tumor size, axillary lymph node status, and histological grade were assessed as classical prognostic factors (14). The Elston-Eillis method of tumor grading was used for histological grading (15), in which a score of 1−3 was assigned for tubule formation, pleomorphism, and mitotic count. The total score could range from 3 to 9, with a total of 3−5 representative of grade 1, a total of 6 or 7 representative of grade 2, and a total of 8 or 9 representative of grade 3.

The expression of ER, PR, c-erbB-2, the p53 tumor suppressor gene, and Ki-67 were assessed as immunohistochemical prognostic factors. A re-cut of the corresponding paraffin block was immunostained with commercially available antibodies to ER (Dako, Glostrup, Denmark), PR (Dako, Glostrup, Denmark), c-erbB-2 (Novocastra, Newcastle, UK), p53 (Dako, Glostrup, Denmark) and Ki-67 (Zymed, San Francisco, CA). The cutoff point for ER and PR positive expression was 10%. Positive expression of

p53 was accepted in any case presenting with well-defined nuclear staining. The c-erbB-2 expression was semiquantitatively assessed as follows: 0 for no membranous staining, 1+ for weak uneven membranous staining in some of the tumor cells, 2+ for weak to moderate membranous staining in a large number of tumor cells, and 3+ for distinctive membranous staining in almost all of the tumor cells. The cutoff point for Ki-67 positve expression was 20%.

Table 1. Correlation between MR Findings and Classical Prognostic Factors

MR Findings	Tumor Size (cm)			Lymph Node Status				Histological Grade		
	≤2.0	2.1–5.0	> 5.0	0	1–3	4–9	≥10	1	2	3
Type										
Mass	76 (39)	91 (47)	3 (2)	100 (52)	50 (26)	12 (6)	8 (4)	15 (8)	70 (36)	85 (44)
Non-Mass	14 (7)	10 (5)	⋯	17 (9)	5 (3)	1 (1)	1 (1)	⋯	8 (4)	16 (8)
P value	0.18 †			0.37 †				0.07 †		
Shape of Mass										
Oval	6 (4)	2 (1)	⋯	3 (2)	4 (2)	1 (1)	⋯	1 (1)	2 (1)	5 (3)
Lobulated	22 (13)	31 (18)	1 (1)	33 (19)	16 (9)	3 (2)	2 (1)	5 (3)	17 (10)	32 (19)
Irregular	48 (28)	58 (34)	2 (1)	64 (38)	30 (18)	8 (5)	6 (4)	9 (5)	51 (30)	48 (28)
P value	0.46 †			0.96 †				0.21 †		
Margin of Mass										
Irregular	42 (25)	61 (36)	2 (1)	64 (38)	31 (18)	7 (4)	3 (2)	4 (2)	29 (17)	72 (42)
Spiculated	34 (20)	30 (18)	1 (1)	36 (21)	19 (11)	5 (3)	5 (3)	11 (7)	41 (24)	13 (8)
P value	0.13 †			0.21 †				< 0.001 †		
Internal Enhancement Pattern of Mass										
Heterogeneous	48 (28)	36 (21)	2 (1)	53 (31)	20 (12)	6 (3)	7 (4)	8 (5)	54 (32)	24 (14)
Rim	28 (17)	55 (33)	1 (1)	47 (28)	30 (18)	6 (4)	1 (1)	7 (4)	16 (9)	61 (36)
P value	0.009 †			0.52 †				< 0.001 †		
Curve Type										
Persistent	9 (5)	4 (2)	⋯	8 (4)	3 (2)	⋯	2 (1)	⋯	9 (5)	4 (2)
Plateau	49 (25)	48 (25)	1 (1)	59 (30)	29 (15)	4 (2)	6 (3)	13 (7)	45 (23)	40 (21)
Washout	32 (17)	49 (25)	2 (1)	50 (26)	23 (12)	9 (5)	1 (1)	2 (1)	24 (12)	57 (29)
P value	0.02 †			0.56 †				< 0.001 †		
Peak Time (sec)										
84	21 (11)	30 (16)	⋯	29 (15)	17 (9)	5 (3)	⋯	3 (2)	17 (9)	31 (16)
168	46 (24)	52 (27)	3 (2)	61 (31)	27 (14)	6 (3)	7 (4)	8 (4)	36 (19)	57 (29)
252	14 (7)	15 (8)	⋯	19 (10)	8 (4)	2 (1)	⋯	4 (2)	16 (8)	9 (5)
336	9 (5)	4 (2)	⋯	8 (4.1)	3 (1.5)	⋯	2 (1.0)	⋯	9 (4.6)	4 (2.1)
P value	0.14 †			0.96 †				0.02 †		
Enhancement Ratio*										
≤100	10 (5)	6 (3)	⋯	12 (6)	3 (2)	1 (1)	⋯	3 (2)	7 (4)	6 (3)
101–150	28 (14)	17 (9)	⋯	22 (11)	19 (10)	2 (1)	2 (1)	5 (3)	19 (10)	21 (11)
151–200	22 (11)	30 (16)	1 (1)	32 (17)	13 (7)	6 (3)	2 (1)	3 (2)	24 (12)	26 (13)
201–250	20 (10)	33 (17)	1 (1)	33 (17)	15 (8)	3 (2)	3 (2)	3 (2)	19 (10)	32 (17)
> 250	10 (5)	15 (8)	1 (1)	18 (9)	5 (3)	1 (1)	2 (1)	1 (1)	9 (5)	16 (8)
P value	0.005 †			0.95 †				0.19 †		
Initial Slope †										
≤1.0	43 (22)	33 (17)	1 (1)	50 (26)	21 (11)	2 (1)	4 (2)	11 (6)	37 (19)	29 (15)
1.1–1.5	25 (13)	33 (17)	1 (1)	31 (16)	17 (9)	7 (4)	4 (2)	⋯	25 (13)	34 (30)
1.6–2.0	9 (5)	12 (6)	1 (1)	12 (6)	9 (5)	⋯	1 (1)	2 (1)	5 (3)	15 (8)
2.1–2.5	5 (3)	9 (5)	⋯	9 (5)	2 (1)	3 (2)	⋯	1 (1)	4 (2)	9 (5)
> 2.5	8 (4)	14 (7)	⋯	15 (8)	6 (3)	1 (1)	⋯	1 (1)	7 (4)	14 (7)
P value	0.08 †			0.66 †				0.006 †		

Note.—Except for *p* values, data are number of lesions; data in parentheses are percentage.

* Signal intensity after contrast injection −baseline signal intensity/baseline signal intensity ×100%.

† Enhancement ratio/peak time.

‡ Linear-by-linear association test.

Statistical Analysis

For univariate analysis, to test whether there was a difference between categorical variables, the Pearson χ^2-test for two by two crosstabs and the linear-by-linear association test for more than two variables in ordinal scale were performed. In order to find the most significant and

Table 2. Correlation between MR Findings and Immunohistochemical Prognostic Factors

MR Findings	ER		PR		p53		c-erbB-2				Ki-67	
	+	–	+	–	–	+	0	1+	2+	3+	–	+
Type												
Mass	107 (55)	63 (32)	101 (52)	69 (36)	49 (25)	121 (62)	101 (52)	35 (18)	15 (8)	19 (10)	102 (53)	68 (35)
Non-Mass	16 (8)	8 (4)	15 (8)	9 (5)	5 (3)	19 (10)	12 (6)	4 (2)	3 (2)	5 (3)	17 (9)	7 (4)
P value	0.72†		0.77†		0.41†		0.16§				0.31†	
Shape of Mass												
Oval	3 (2)	5 (3)	2 (1)	6 (4)	3 (2)	5 (3)	4 (2)	2 (1)	…	2 (1)	5 (3)	3 (2)
Lobulated	29 (17)	25 (15)	29 (17)	25 (15)	14 (8)	40 (23)	35 (21)	8 (5)	6 (4)	5 (3)	32 (19)	22 (13)
Irregular	75 (44)	33 (19)	70 (41)	38 (22)	32 (19)	76 (45)	62 (37)	25 (15)	9 (5)	12 (7)	65 (38)	43 (25)
P value	0.01§		0.02§		0.96§		0.92§				1.00§	
Margin of Mass												
Irregular	59 (35)	46 (27)	54 (32)	51 (30)	30 (18)	75 (44)	61 (36)	18 (11)	9 (5)	17 (10)	52 (31)	53 (31)
Spiculated	48 (28)	17 (10)	47 (28)	18 (11)	19 (11)	46 (27)	40 (24)	17 (10)	6 (4)	2 (4)	50 (29)	15 (9)
P value	0.02†		0.007†		0.93†		0.07§				< 0.001†	
Internal Enhancement Pattern of Mass												
Heterogeneous	65 (38)	21 (12)	65 (38)	21 (12)	25 (15)	61 (36)	48 (28)	26 (15)	8 (5)	4 (2)	62 (37)	24 (14)
Rim	42 (25)	42 (25)	1 (1)	48 (28)	24 (14)	60 (35)	53 (31)	9 (5)	7 (4)	15 (9)	40 (24)	44 (26)
P value	0.001†		<0.001†		0.94†		0.25§				0.001†	
Curve Type												
Persistent	8 (4)	5 (3)	7 (4)	6 (3)	5 (3)	8 (4)	7 (4)	3 (2)	2 (1)	1 (0)	10 (5)	3 (2)
Plateau	68 (35)	30 (16)	64 (33)	34 (18)	28 (14)	70 (36)	60 (31)	23 (12)	6 (3)	9 (5)	74 (38)	24 (12)
Washout	47 (24)	36 (19)	45 (23)	38 (20)	21 (11)	62 (32)	46 (24)	13 (7)	10 (5)	14 (7)	35 (18)	48 (25)
P value	0.19§		0.35§		0.36§		0.18§				< 0.001§	
Peak Time (sec)												
84	26 (13)	25 (13)	24 (12)	27 (14)	15 (8)	36 (19)	34 (18)	8 (4)	…	9 (5)	22 (11)	29 (15)
168	71 (37)	39 (16)	64 (33)	37 (19)	25 (13)	76 (39)	54 (28)	21 (11)	14 (7)	12 (6)	63 (33)	38 (20)
252	18 (9)	11 (6)	21 (11)	8 (4)	9 (5)	20 (10)	18 (9)	7 (4)	2 (1)	2 (1)	24 (12)	5 (3)
336	8 (4)	5 (3)	7 (4)	6 (3)	5 (3)	8 (4)	7 (4)	3 (2)	2 (1)	1 (1)	10 (5)	3 (2)
P value	0.33§		0.13§		0.58§		0.93§				< 0.001§	
Enhancement Ratio*												
≤ 100	9 (5)	7 (4)	8 (4)	8 (4)	7 (4)	9 (5)	9 (5)	4 (2)	1 (1)	2 (1)	9 (5)	7 (4)
101–150	28 (14)	17 (9)	26 (13)	19 (10)	11 (6)	34 (18)	26 (13)	14 (7)	1 (1)	4 (2)	30 (16)	15 (8)
151–200	36 (19)	17 (9)	34 (18)	19 (10)	16 (8)	37 (19)	34 (18)	8 (4)	5 (3)	6 (3)	34 (18)	19 (10)
201–250	36 (19)	18 (9)	35 (18)	19 (10)	14 (7)	40 (21)	26 (13)	10 (5)	9 (5)	9 (5)	29 (15)	25 (13)
> 250	14 (7)	12 (6)	13 (7)	13 (7)	6 (3)	20 (10)	18 (9)	3 (2)	2 (1)	3 (2)	17 (9)	9 (5)
P value	0.96§		0.84§		0.33§		0.45§				0.72§	
Initial Slope†												
≤ 1.0	52 (27)	25 (13)	48 (25)	29 (15)	22 (11)	55 (28)	43 (22)	20 (10)	5 (3)	9 (5)	58 (30)	19 (10)
1.1–1.5	40 (21)	19 (10)	39 (20)	20 (10)	16 (8)	43 (22)	32 (17)	11 (6)	11 (6)	5 (3)	33 (17)	26 (13)
1.6–2.0	11 (6)	11 (6)	12 (6)	10 (5)	8 (4)	14 (7)	15 (8)	2 (1)	2 (1)	3 (2)	11 (6)	11 (6)
2.1–2.5	7 (4)	7 (4)	6 (3)	8 (4)	2 (1)	12 (6)	11 (6)	…	…	3 (2)	7 (4)	7 (4)
> 2.5	13 (7)	9 (5)	11 (6)	11 (6)	6 (3)	16 (8)	12 (6)	6 (3)	…	4 (2)	10 (5)	12 (6)
P value	0.16§		0.12§		0.73§		0.98§				0.003§	

Note.—Except for *p* values, data are number of lesions; data in parentheses are percentage.

* Signal intensity after contrast injection – baseline signal intensity/baseline signal intensity ×100%.

† Enhancement ratio/peak time.

‡ Pearson χ^2-test.

§ Linear-by-linear association test.

independent relationship, multivariate analyses were performed. Variables found to be significant by univariate analysis were tested in regression models. For dichotomous dependent variables, a binary logistic regression with forward-likelihood-ratio covariate selection method was performed. Logistic regression was applied to analyze the effects of the different MR parameters as follows. Tumor size by grouping 2 cm or less than 2 cm versus more than 2 cm, by grouping the histological grade of grade 1 and grade 2 lesions versus grade 3 lesions, by grouping expression of ER and PR positive versus negative, by grouping the expression of c-erbB-2 with 0, 1+, 2+, versus the 3+ category, by grouping expression of p53 negative versus positive, and by grouping Ki-67 negative versus positive.

A p value less than 0.05 was considered as statistically significant. The statistical analyses were performed with statistical software (SPSS for Microsoft Windows, version 10.0; SPSS, Chicago, IL).

RESULTS

Imaging Analysis

Of the 194 cases of invasive ductal carcinoma NOS, there were 170 (88%) mass lesions and 24 (12%) non-mass enhancement lesions. Of the 170 masses, there were eight (5%) oval shape, 54 (32%) lobulated shape, and 108 (64%) irregular shape lesions. There were 105 (62%) irregular margin, and 65 (38%) spiculated margin lesions. There were 86 (51%) cases of heterogeneous enhancement, and 84 (49%) cases of rim enhancement. Round shape, smooth margin, and homogeneous enhancement were not noted. Of the 194 invasive ductal carcinomas NOS, the curve types were persistent in 13 (7%) lesions, plateau in 98 lesions (51%), and washout in 83 (43%) lesions. A peak time occurring at the first postcontrast phase was seen for 51 (26%) lesions, at the second

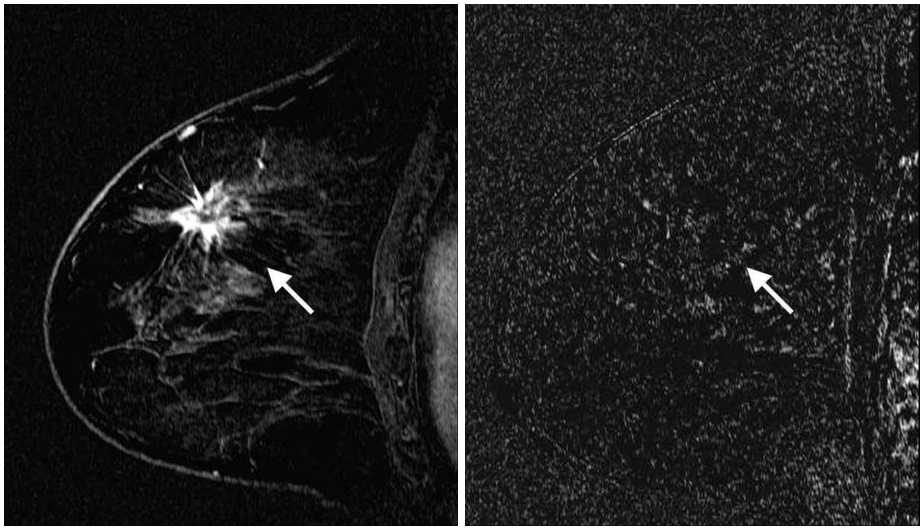

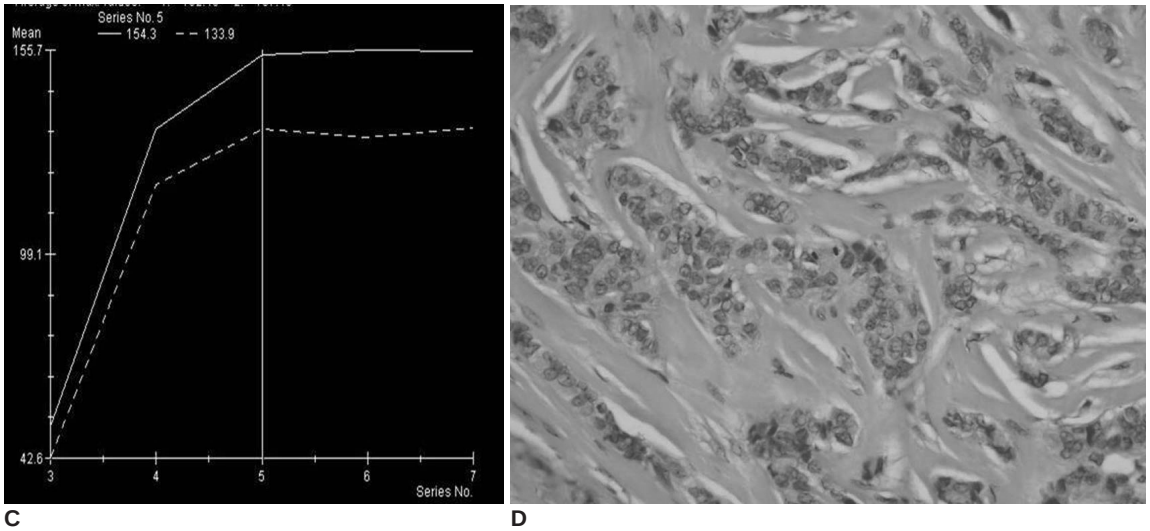

Fig. 1. A 56-year-old woman with invasive ductal carcinoma not otherwise specified of histological grade 1, ER (+), PR (+), Ki-67 (−).
A. Sagittal standard subtracted fast low-angle shot MR image shows an irregular mass with a spiculated margin (arrow).
B. Sagittal reverse subtracted fast low-angle shot MR image shows non-washout kinetics (arrow).
C. Time-signal intensity curve shows plateau late enhancement.
D. Photomicrograph shows high proportional tubule formation, low nuclear pleomorphism, and a low mitotic count (Hematoxylin & Eosin staining, ×400).

postcontrast phase was seen for 101 (52%) lesions, at the third postcontrast phase was seen for 29 (15%) lesions, and at the fourth postcontrast phase was seen for 13 (7%) lesions.

The enhancement ratio ranged from 42–533% (mean 193 ± 74%). The initial slope ranged from 0.22–6.35 (mean 1.36 ± 0.84) (Tables 1, 2).

Histopathological Analysis

Tumor size ranged from 0.1–6.0 cm (mean 2.2 ± 1.0 cm). The number of axillary lymph node metastasis ranged from 0–29 (mean 1.6). Of the tumors, 60% (117 of 194) had no axillary lymph node metastasis and 29% (55 of 194) had one to three metastatic lymph nodes. Of the tumors, 52% (101 of 194) were assessed as high grade and 48% (93 of 194) were low grade (Table 1). Of the tumors, 63% (123 of 194) were ER positive, 60% (116 of 194) were PR positive, 72% (140 of 194) were p53 positive, and 39% (75 of 194) were Ki-67 positive. In 58% (113 of 194) of the tumors no expression of c-erbB-2 protein was evident, 20% (39 of 194) were 1+, 9% (18 of 194) were 2+, and 12% (24 of 194) were 3+ (Table 2).

Statistical Analysis

By univariate analysis, the shape of the mass was significantly associated with the ER ($p = 0.01$), and PR expression status ($p = 0.02$). The margin of mass was significantly associated with the histological grade ($p < 0.001$), expression of ER ($p = 0.02$), expression of PR ($p = 0.007$), and Ki-67 status ($p < 0.001$). The internal enhancement pattern was significantly associated with tumor size ($p = 0.009$), histological grade ($p < 0.001$), expression of ER ($p = 0.001$), expression of PR ($p < 0.001$) and Ki-67 status ($p = 0.001$). The curve type was significantly associated with tumor size ($p = 0.02$), histological grade ($p < 0.001$) and Ki-67 status ($p < 0.001$). Of the parameters of the initial

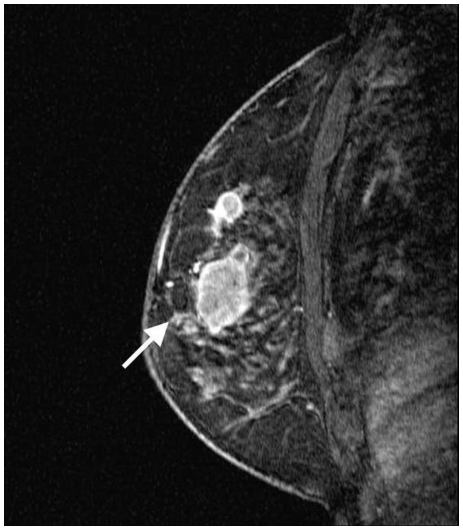

A

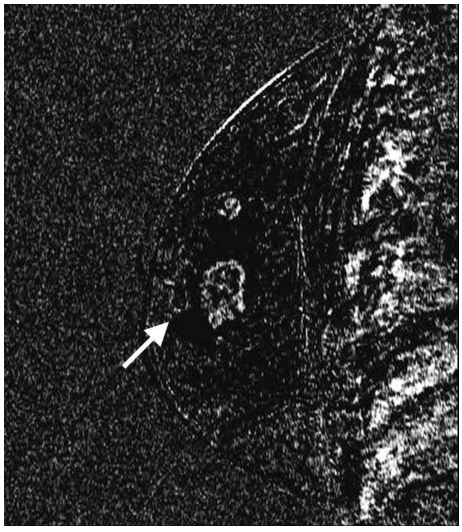

B

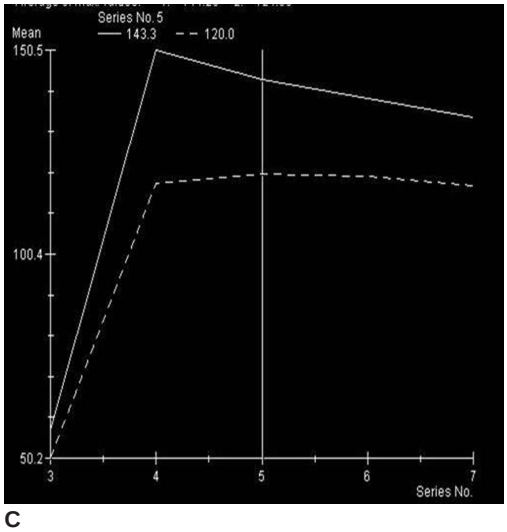

C

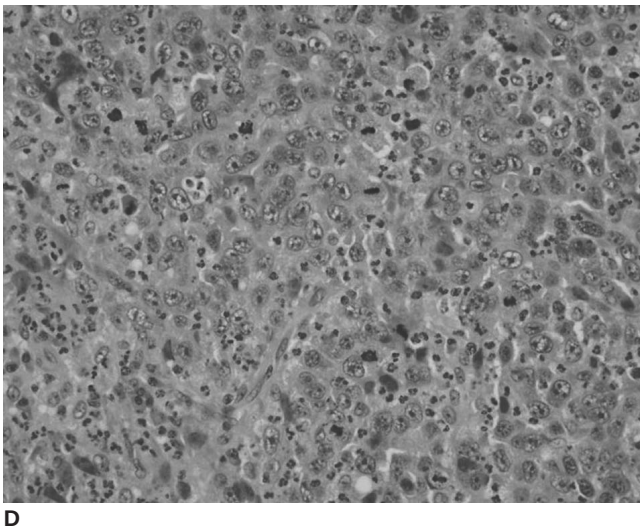

D

Fig. 2. A 48-year-old woman with invasive ductal carcinoma not otherwise specified of histological grade 3, ER (–), PR (–), Ki-67 (+).
A. Sagittal standard subtracted fast low-angle shot MR image shows a lobulated mass with rim enhancement (arrow).
B. Sagittal reverse subtracted fast low-angle shot MR image shows washout kinetics (arrow).
C. Time-signal intensity curve shows washout late enhancement.
D. Photomicrograph shows minimal tubule formation, high nuclear pleomorphism, and a high mitotic count (Hematoxylin & Eosin staining, ×400).

phase, peak time was significantly associated with the histological grade ($p = 0.02$) and Ki-67 status ($p < 0.001$). The enhancement ratio was significantly associated with tumor size ($p = 0.005$). The initial slope was significantly associated with the histological grade ($p = 0.006$), and Ki-67 status ($p = 0.003$). A correlation was not found between MR features with lymph node status, p53 status and c-erbB-2 status (Tables 1, 2).

Parameters found to be significant by univariate analysis were selected for logistic regression analysis. The internal enhancement pattern of mass, curve type, and enhancement ratio entered into the regression model of tumor size. The margin, internal enhancement pattern of mass, curve type, peak time, and initial slope entered into the regression model of histological grade. The shape, margin, and internal enhancement pattern of mass entered into the regression model of ER and PR status respectively. The margin, internal enhancement pattern of mass, curve type, peak time, and initial slope entered into the regression model of Ki-67 status. By multivariate analysis, spiculated margin was a significant, independent predictor of a lower histological grade ($p < 0.001$), and lower expression of Ki-67 ($p = 0.007$) (Fig. 1). Rim enhancement was a significant, independent predictor of a higher histological grade ($p < 0.001$), negative expression of ER ($p = 0.001$), negative expression of PR ($p < 0.001$) (Fig. 2), and a larger tumor size ($p = 0.006$). A washout curve may predict higher a Ki-67 status ($p = 0.05$). An enhancement ratio more than 200% may predict a larger tumor size ($p = 0.05$) (Table 3).

DISCUSSION

In this study, a spiculated margin of breast cancer on high spatial resolution dynamic MR was able to predict a lower histological grade and lower Ki-67 status. This result was consistent with previous studies. It is well-known that high grade breast cancers show circumscribed margins because of their high cellularity and rich hyaluronic acid

Table 3. Results of Logistic Regression Analysis*

Included Variables	B**	S.E.††	Odds ratio	*P* value
For Tumor Size†				
Rim enhancement	0.90	0.33	2.45	0.006
Enhancement ratio				0.05
101–150	0.46	0.69	1.58	0.51
151–200	1.19	0.68	3.28	0.08
201–250	1.48	0.68	4.39	0.04
> 250	1.59	0.76	4.91	0.04
For Histological Grade‡				
Spiculated margin	-1.83	0.40	0.16	< 0.001
Rim enhancement	1.50	0.37	4.46	< 0.001
For ER§				
Rim enhancement	1.13	0.33	3.01	0.001
For PR‖				
Rim enhancement	1.42	0.33	4.13	< 0.001
For Ki-67¶				
Spiculated margin	-0.99	0.37	0.37	0.007
Curve type				
Persistent curve	…		…	0.001
Plateau curve	0.45	0.83	1.57	0.59
Washout curve	1.65	0.83	5.23	0.05

Note.—* Binary logistic regression with likelihood-ratio covariate selection method.

† Dependent variable was tumor size with grouping ≤ 2 cm vs > 2 cm; independent variables were internal enhancement pattern of mass, curve type, and enhancement ratio.

‡ Dependent variable was histological grade with grouping 1 and 2 vs 3; independent variables were margin of mass, internal enhancement pattern of mass, curve type, peak time, and initial slope.

§ Dependent variable was ER with grouping positive vs negative; independent variables were shape of mass, margin of mass, and internal enhancement pattern of mass.

‖ Dependent variable was PR with grouping positive vs negative; independent variables were shape of mass, margin of mass, and internal enhancement pattern of mass.

¶ Dependent variable was Ki-67 with grouping negative vs positive; independent variables were margin of mass, internal enhancement pattern of mass, curve type, peak time, and initial slope.

** Regression coefficients.

†† Standard error of the estimate.

extracelluar matrix and inflammatory host reaction, whereas low grade cancers show a spiculated margin because of their low cellularity, rich collagen matrix and desmoplastic host reaction (16, 17). However, this finding differed from that reported by Szabó et al. (4) who found that there was no correlation between the margin of a breast cancer and prognostic factors. This difference might be due to the different resolution of the MR imaging. Spatial resolution in this study (0.29 mm^2 pixel size, 1 mm thickness, and unilateral sagittal scan) was higher than in the Szabó et al. study (3.6 mm^2 pixel size, 2.2 mm thickeness, bilateral axial scan). A high resolution image is necessary for an accurate analysis of the margin.

Another important result of this study was that rim enhancement was a significant, independent predictor of a higher histological grade ($p < 0.001$), negative expression of ER ($p = 0.001$), negative expression of PR ($p < 0.001$), and a larger tumor size ($p = 0.006$). The mechanism of rim enhancement of breast cancer as seen on MR imaging can be explained by high angiogenesis in the periphery of the tumor, central necrosis, and central desmoplasia (6, 18−20). There have been several studies showing a correlation between rim enhancement and a higher histological grade, negative expression of ER, higher expression of Ki-67, lymph node status (4−6, 13), and the percentage of cells in DNA-S phase, a measure of cellular proliferative activity (21). Although Mussurakis et al. (3) reported that there was no correlation between rim enhancement and histopathological prognostic factors, results of this study suggest that there is a correlation between rim enhancement and poor prognostic factors.

The parameters of the initial enhancement phase (2 to 3 minutes after contrast injection or when the curve starts to change) had a role in the differentiation of benign and malignant tumors of the breast. Faster and stronger enhancement suggests a malignant lesion. However, there has been a considerable overlap between benign and malignant tumors in the initial enhancement parameters (22). The parameter of delayed enhancement phase determines the type of enhancement curve. In general, benign lesions show a persistent curve and malignant lesions show a washout curve, and a plateau curve can be seen in both benign and malignant lesions (1, 2). Controversies exist for the relationship between kinetic parameters and prognostic factors. There have been several reports about the significant correlation between the enhancement ratio and the axillary lymph node status or histological grade (7, 8) or high cellular proliferation (8). There have been reports about a significant correlation between washout and higher tumor grade (4, 8) or a higher histological grade, positive Ki-67 (4, 6, 13), and negative ER status (4). Tuncbilek et al. (11) also reported that parameters of the initial enhancement phase were correlated with grade. However, Stomper et al. (9) reported that time-intensity curves showed no significant correlation with pathological size, nodal status, or the hormone receptor status of an invasive carcinoma. Fischer et al. (10) reported that there was no correlation between the enhancement ratio and the histological type of carcinoma, grade, and lymph node status. Among these kinetic parameters, our study demonstrated that the washout curve was a significant, independent predictor of Ki-67 positive expression, suggesting higher proliferative activity and that most of parameters of initial enhancement phase could not reflect prognostic factors.

This study has some limitations. First, we did not follow patients. To draw a prognostic significance from our analysis, follow-up of patients and multifactorial survival analysis are required. Second, MR images were interpreted by two observers in consensus, so interobserver variability could not be determined.

There are some differences in this study from previous studies. First, our study included only patients with invasive ductal carcinoma NOS. Thus, we excluded bias from the histopathological variability. Second, highly spatial and temporal resolution images were obtained using a 1.5 T dynamic 3D MR instrument, allowing the morphologic and kinetic features of breast cancers to be meticulously analyzed. Finally, we used the BI-RADS-MR imaging lexicon enabling a standardized communication.

In conclusion, of the BI-RADS-MR features, a spiculated margin may predict a favorable prognosis, whereas rim enhancement and washout may predict an unfavorable prognosis of breast cancer. These MR features can be used to select subgroups of breast cancers with different biological behavior.

References

1. Kuhl CK, Mielcareck P, Klaschik S, Leutner C, Wardelmann E, Gieseke J, et al. Dynamic breast MR imaging: are signal intensity time course data useful for differential diagnosis of enhancing lesions? *Radiology* 1999;211:101-110
2. Orel SG. Differentiating benign from malignant enhancing lesions identified at MR imaging of the breast: are time-signal intensity curves an accurate predictor? *Radiology* 1999;211:5-7
3. Mussurakis S, Gibbs P, Horsman A. Peripheral enhancement and spatial contrast uptake heterogeneity of primary breast tumors: quantitative assessment with dynamic MRI. *J Comput Assist Tomogr* 1998;22:35-46
4. Szabó BK, Aspelin P, Kristoffersen Wiberg M, Tot T, Bone B. Invasive breast cancer: correlation of dynamic MR features with prognostic factors. *Eur Radiol* 2003;13:2425-2435
5. Jinguji J, Kajiya Y, Kamimura K, Nakajo M, Sagara Y, Takahama T, et al. Rim enhancement of breast cancers on contrast-enhanced MR imaging: relationship with prognostic

factors. *Breast Cancer* 2006;13:64-73
6. Teifke A, Behr O, Schmidt M, Victor A, Vomweg TW, Thelen M, et al. Dynamic MR imaging of breast lesions: correlation with microvessel distribution pattern and histologic characteristics of prognosis. *Radiology* 2006;239:351-360
7. Mussurakis S, Buckley DL, Horsman A. Dynamic MR imaging of invasive breast cancer: correlation with tumor grade and other histologic factors. *Br J Radiol* 1997;70:446-451
8. Bone B, Aspelin P, Bronge L, Veress B. Contrast-enhanced MR imaging as a prognostic indicator of breast cancer. *Acta Radiol* 1998;39:279-284
9. Stomper PC, Herman S, Klippenstein DL, Winston JS, Edge SB, Arredondo MA, et al. Suspect breast lesions: findings at dynamic gadolinium-enhanced MR imaging correlated with mammographic and pathologic features. *Radiology* 1995;197:387-395
10. Fischer U, Kopka L, Brinck U, Korabiowska M, Schauer A, Grabbe E. Prognostic value of contrast-enhanced MR mammography in patients with breast cancer. *Eur Radiol* 1997;7:1002-1005
11. Tuncbilek N, Karakas HM, Okten OO. Dynamic magnetic resonance imaging in determining histopathological prognostic factors of invasive breast cancers. *Eur J Radiol* 2005;53:199-205
12. American College of Radiology. *Breast Imaging Reporting and Data System- Magnetic Resonance Imaging,* 1st ed. Reston, Va: American College of Radiology, 2003
13. Lee SH, Cho N, Chung HK, Kim SJ, Cha JH, Cho KS, et al. Breast MR imaging: correlation of high resolution dynamic MR findings with prognostic factors. *J Korean Radiol Soc* 2005;52:355-361(Korean)
14. Elston CW, Ellis IO, Pinder SE. Pathologic prognostic factors in breast cancer. *Crit Rev Oncol Hematol* 1999;31:209-223
15. Elston CW, Ellis IO. Pathological prognostic factors in breast cancer. I. The value of histological grade in breast cancer: experience from a large study with long-term follow-up. *Histopathology* 1991;19:403-410
16. Stavros AT, Thickman D, Rapp CL, Dennis MA, Parker SH, Sisney GA. Solid breast nodule: use of sonography to distinguish between benign and malignant lesions. *Radiology* 1995;196:123-134
17. Stavros AT. *Malignant solid breast nodules: specific type*. In: Stavros AT, ed. *Breast ultrasound,* 1st ed. Philadelphia, Pa: Lippincott Williams & Wilkins, 2004:597-688
18. Buadu LD, Murakami J, Murayama S, Hashiguchi N, Sakai S, Masuda K, et al. Breast lesions: correlation of contrast medium enhancement patterns on MR images with histopathologic findings and tumor angiogenesis. *Radiology* 1996;200:639-649
19. Buckley DL, Drew PJ, Mussurakis S, Monson JR, Horsman A. Microvessel density of invasive breast cancer assessed by dynamic Gd-DTPA enhanced MRI. *J Magn Reson Imaging* 1997;7:461-464
20. Matsubayashi R, Matsuo Y, Edakuni G, Satoh T, Tokunaga O, Kudo S. Breast masses with peripheral rim enhancement on dynamic contrast-enhanced MR images: correlation of MR findings with histologic features and expression of growth factors. *Radiology* 2000;217:841-848
21. Stomper PC, Herman S, Klippenstein DL, Winston JS, Budnick RM, Stewart CC. Invasive breast carcinoma: analysis of dynamic magnetic resonance imaging enhancement features and cell proliferative activity determined by DNA S-phase percentage. *Cancer* 1996;77:1844-1849
22. Heywang-Kobrunner SH. Contrast enhanced magnetic resonance imaging of the breast. *Invest Radiol* 1994;29:94-104